J. Fluid Mech. (1992), *vol.* 243, *pp.* 155–169
Printed in Great Britain

Weakly nonlinear theory of the alternation of modes in a circular shear flow

By S. M. CHURILOV AND I. G. SHUKHMAN
SibIZMIR, Irkutsk 33, P.O. Box 4026, 664033 Russia

(Received 20 August 1990 and in revised form 1 July 1991)

Experimental investigations on the origin and evolution of structure in circular shear flows, made under different conditions by different groups of authors, reveal a number of common regularities. (i) When the difference $\Delta\Omega$ between the angular velocities of the centre and the periphery is smaller than a certain critical value $(\Delta\Omega)_c$, the flow is axisymmetric. (ii) When $\Delta\Omega = (\Delta\Omega)_c$, a pattern appears consisting of m_c vortices. (iii) With a subsequent adiabatic growth of $\Delta\Omega$ (at a certain $(\Delta\Omega)^+_{m_c} > (\Delta\Omega)_c$), transition to a pattern with $m_c - 1$ vortices occurs, but a pattern with $m_c + 1$ vortices never arises (although in terms of linear theory the modes $m_c - 1$ and $m_c + 1$ are equivalent). Subsequent growth of $\Delta\Omega$ leads to the transition $(m_c - 1) \to (m_c - 2)$, etc. (iv) As $\Delta\Omega$ decreases, a cascade of inverse transitions of the form $m - 1 \to m$ up to $m = m_c$ occurs, and the transition $m - 1 \to m$ proceeds at a smaller value of $\Delta\Omega$ compared with the transition $m \to m - 1$, i.e. hysteresis occurs.

This paper offers a weakly nonlinear theory which makes it possible to describe the change of the order of symmetry of the wave pattern (number of vortices) with a change of $\Delta\Omega$ and to ascertain conditions under which the above regularities occur. Some particular examples of the calculation of several models of shear flows are given, and it is shown that direct transitions $(m \to m - 1)$ can be described in terms of a weakly nonlinear theory only for flows with a sufficiently large curvature of the shear layer, i.e. when $D \equiv L/R = O(1)$, where L is the width of the shear layer, and R is its radius, and at not too large m ($m_c = 4, 5$). If $D \ll 1$, a description of direct transitions requires a strongly nonlinear theory and is beyond the scope of this paper. Inverse transitions $(m - 1 \to m, m \leqslant m_c)$ admit a weakly nonlinear treatment at any D.

1. Introduction

To date, extensive experimental material has been accumulated on the formation and evolution of large-scale structure in circular shear flows of a thin layer of liquid or gas. Investigations have been made under different physical conditions on quite different devices. Studies have been made of flows both under a rigid lid (for example, Niino & Misawa 1984; Rabaud & Couder 1983; Chomaz *et al.* 1988) and with a free surface (Nezlin *et al.* 1990; Nezlin & Snezhkin 1990; Dolzhanskiĭ, Krymov & Manin 1990). A shear flow (differential rotation) of the medium was usually created mechanically, through the rotation with different angular velocities of either (i) the central part $(0 < r < R)$ and the periphery $(r > R)$ of the bottom and of the lid, if any (for example, Niino & Misawa 1984; Rabaud & Couder 1983; Chomaz *et al.* 1988; Nezlin *et al.* 1990) or (ii) of the annular region $(R_1 < r < R_2)$ and of the remaining part of the bottom (for example, Nezlin *et al.* 1990). However, in some experiments the

flow was produced in a fixed vessel by external forces, for example by Ampere's force that arises when a radial current passes through conducting fluid in a vertical axisymmetric magnetic field $B(r)$ (Dolzhanskiĭ *et al.* 1990).

An axisymmetric quasi-two-dimensional flow is produced in either manner and can be conveniently represented as the sum of the mean rotation and the shear flow itself:

$$v_\phi = \bar{\Omega} r + V u(r),$$

where $u(r)$ is specified by the design of the device, and the value of velocity shear V can be varied, by varying the difference $\Delta\Omega$ of angular velocities of different parts of the bottom (in the mechanical method), or the parameter controlling the value of an external force (current in the case of Ampere's force).

Thus, controlling the flow is reduced to varying the Reynolds number which can be determined in two ways: either from viscosity, or from Ekman friction (Pedlosky 1979):

$$Re = \frac{VL}{\nu} \quad \text{and} \quad Re_\lambda = \frac{V}{L\tilde{\lambda}}, \tag{1.1}$$

where ν is the viscosity coefficient, $\tilde{\lambda} = O(\nu/h^2)$ is the coefficient of Ekman friction, $L = (\max|\mathrm{d}u/\mathrm{d}r|)^{-1}$ is the horizontal scale of the shear layer, and h is the thickness of the layer of fluid ($h \ll h_E = (\nu/\bar{\Omega})^{\frac{1}{2}}$). It is easy to see that their ratio $\rho = Re_\lambda/Re = O(h^2/L^2)$ is also specified by the design of the device and, in the course of each experiment, remains fixed. In the mechanical method of producing the flow, L and h are closely related, $L/h = \text{const} = O(1)$, and so $\rho = O(1)$. In flows produced by external forces, L and h are independent, and ρ can be arbitrary; in most such experiments $\rho \ll 1$, which permits us to neglect the viscosity compared with Ekman friction. Therefore, Re_λ (or $\lambda = Re_\lambda^{-1}$) is a more convenient control parameter.

The experiments, made under different conditions, have revealed a number of common behaviour features of the flows with a change of Re_λ. If Re_λ is increased adiabatically (very slowly), the axisymmetrical flow becomes unstable when $Re_\lambda = Re_{\lambda C}$ and a flow with m vortices appears, with m corresponding to the most unstable, or fundamental mode of linear theory. The disturbance energy increases proportionally with the super-criticality $(Re_\lambda - Re_{\lambda C})$, which indicates a soft regime of excitation through a Hopf bifurcation (Dolzhanskiĭ *et al.* 1990). When reaching a certain $Re_\lambda = Re^+_{\lambda m_C}$, this flow also becomes unstable and a transition to a flow with $m = m_C - 1$ vortices (to the mode $m_C - 1$) occurs. With a further increase of Re_λ, the mode $m_C - 1$ is replaced by the mode $m_C - 2$, and so on. This is a direct transition cascade. If, however, Re_λ is decreased adiabatically, there is an inverse transition cascade of $m \to m+1$ type. In other words, a flow with $m < m_C$ vortices is stable in a certain interval $Re^-_{\lambda m} < Re_\lambda < Re^+_{\lambda m}$. When the lower or upper boundary is reached, the transitions $m \to m+1$ or $m \to m-1$, respectively, occur. A transition is, usually, accomplished abruptly, with hysteresis occurring in the case $Re^-_{\lambda m} < Re^+_{\lambda,m+1}$, i.e. direct and inverse transitions between the modes m and $m+1$ proceed at different values of Re_λ (see figure 1).†

Note two important features observed in all experiments known to us. Firstly, an

† This is the most frequently occurring scenario. In some flows with $\rho \ll 1$ there is a gradual transition $m \rightleftharpoons m+1$ through a mixed state, or a superposition of two modes. In this case $Re^+_{\lambda,m+1} < Re^-_{\lambda m}$, and when Re_λ increases from $Re^+_{\lambda,m+1}$ to $Re^-_{\lambda m}$ the 'weight' of the $(m+1)$ mode decreases from 1 to 0, while the 'weight' of the mth mode increases from 0 to 1 (Dovzhenko & Krymov 1987). In some experiments the results were of probabilistic character: in a direct cascade there were either $m \to m-1$ or $m \to m-2$ transitions, and in an inverse cascade, $m \to m+1$ or $m \to m+2$ transitions occurred, and the probability for either outcome was found to be independent of the variation rate of the control parameter Re_λ (Krymov 1988).

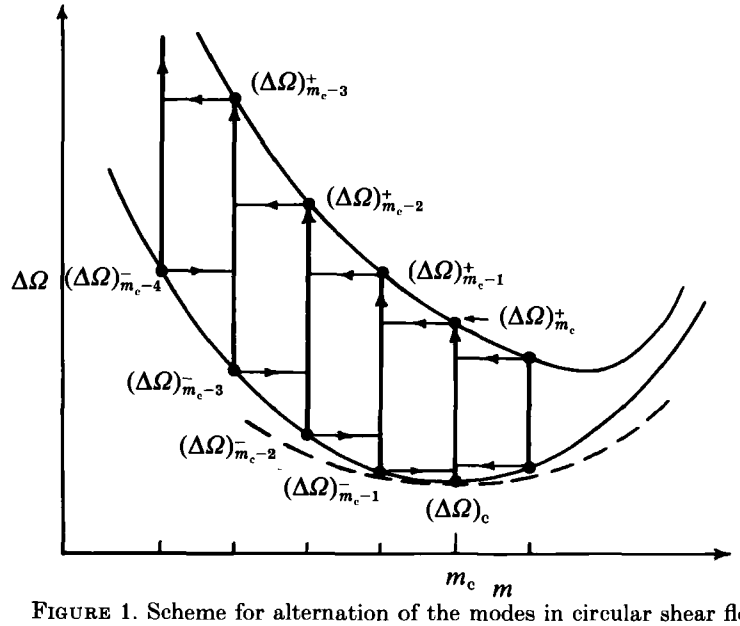

FIGURE 1. Scheme for alternation of the modes in circular shear flows. Dashed line shows the neutral curve of linear stability theory.

adiabatic change of Re_λ is never accompanied by the excitation of a mode with $m > m_C$, although in linear theory $m > m_C$ and $m < m_C$ are equivalent. Secondly, $Re^+_{\lambda m}$ is rather large and, in terms of linear theory, with such Re_λ values, a whole spectrum of modes rather than only the mth and $(m-1)$th modes are unstable, including even more unstable modes than the mth mode, not to mention the $(m-1)$th mode. Consequently, the presence of a well-developed mth mode, when $Re^-_{\lambda m} < Re_\lambda < Re^+_{\lambda m}$, suppresses the development of the other modes.

These properties indicate that the processes under consideration have a nonlinear character and seem to be common to supercritical regimes of development of hydrodynamical instabilities of different types. Similar transitions have been observed when studying convection, baroclinic instability, Couette flow, etc. Many authors use a system of two nonlinearly interacting modes with amplitudes A_1 and A_2 as a weakly nonlinear theoretical model of such processes, which is described by the equations

$$\left.\begin{aligned} \frac{dA_1}{dt} &= \mu_1 A_1 - \tilde{b}_{11}|A_1|^2 A_1 - \tilde{b}_{12}|A_2|^2 A_1, \\ \frac{dA_2}{dt} &= \mu_2 A_2 - \tilde{b}_{21}|A_1|^2 A_2 - \tilde{b}_{22}|A_2|^2 A_2. \end{aligned}\right\} \tag{1.2}$$

In this approximation μ_1 and μ_2 depend linearly on the control parameter

$$\mu_1 = a_1(\lambda_1 - \lambda), \quad \mu_2 = a_2(\lambda_2 - \lambda),$$

and $\tilde{b}_{ik}$ does not depend on λ. For definiteness, it will be assumed that $\lambda_1 > \lambda_2$. Generally speaking, $\tilde{b}_{ik}$ are complex; therefore, it is a convenient to proceed in terms of 'numbers of quasi-particles' $N_i = b_{ii}|A_i|^2$:

$$\left.\begin{aligned} \frac{1}{2}\frac{dN_1}{dt} &= a_1(\lambda_1 - \lambda)N_1 - N_1^2 - b_1 N_1 N_2, \\ \frac{1}{2}\frac{dN_2}{dt} &= a_2(\lambda_2 - \lambda)N_2 - b_2 N_1 N_2 - N_2^2. \end{aligned}\right\} \tag{1.3}$$

Here $b_{ik} = \mathrm{Re}\,(\tilde{b}_{ik})$, $b_1 = b_{12}/b_{22}$, $b_2 = b_{21}/b_{11}$, $b_{11} > 0$, $b_{22} > 0$.

Since the work by Lotka (1925) and Volterra (1931) on the dynamics of populations, equations of types (1.2) and (1.3) have been widely used in different branches of science, including hydrodynamical applications (see, for example, Segel & Stuart 1962; Drazin 1972; Knobloch & Guckenheimer 1983; Moroz & Holmes 1984). In the last two quoted papers a detailed analysis is made and bifurcation diagrams for these equations are constructed. In the present study we shall attempt to ascertain the extent to which the properties of circular shear flows can be interpreted in terms of a weakly nonlinear two-mode model, and what these properties are. Therefore, following Moroz & Holmes (1984) we shall give a brief outline of the results of analysis of (1.3) with applications to our problem (where, in particular, $b_1 > 0$ and $b_2 > 0$).

The system (1.3) has four different equilibria, although with the given μ_1 and μ_2 not all of them necessarily exist. These equilibria are:

C0: $N_1 = 0$, $N_2 = 0$; exists at all μ_1, μ_2. This is a stable sink if μ_1, $\mu_2 < 0$, a saddle if $\mu_1 > 0 > \mu_2$, and an unstable source if μ_1, $\mu_2 > 0$.

C1: $N_1 = \mu_1$, $N_2 = 0$; exists if $\mu_1 > 0$. If $b_2\mu_1 > \mu_2$, this is a stable sink, otherwise it is a saddle.

C2: $N_1 = 0$, $N_2 = \mu_2$; exists if $\mu_2 > 0$. If $b_1\mu_2 > \mu_1$, it is a sink, otherwise it is a saddle.

C3: $N_1 = (\mu_1 - b_1\mu_2)/(1-b_1b_2)$, $N_2 = (\mu_2 - b_2\mu_1)/(1-b_1b_2)$; the existence condition is N_1, $N_2 > 0$. If $d \equiv 1-b_1b_2 < 0$, it is a saddle, otherwise it is a sink.

Equilibria C1 and C2 are 'pure' modes 1 and 2 respectively, and C3 is a mixed mode, 1+2. The transition from one state to the other occurs when λ takes one of the four critical values defined by the relationships:

$$\left.\begin{aligned} &\lambda = \lambda_1: \quad \mu_1 = 0, \text{ C1 appears (disappears)};\\ &\lambda = \lambda_2: \quad \mu_2 = 0, \text{ C2 appears (disappears)};\\ &\lambda = \lambda_{C1}: \quad \mu_2 = b_2\mu_1, \text{ C1 stability changes};\\ \text{and}\quad &\lambda = \lambda_{C2}: \quad \mu_1 = b_1\mu_2, \text{ C2 stability changes}. \end{aligned}\right\} \tag{1.4}$$

It is easy to show that under the transitions from C1, C2 to C3 and vice versa, N_i are continuous, and the transitions between C1 and C2 proceed abruptly and are accompanied by hysteresis (i.e. the transitions C1 → C2 and C2 → C1 occur at different values of λ). According to whether the inequalities

$$b_2 < a_2/a_1, \tag{1.5a}$$

$$b_1 > a_1/a_2, \tag{1.5b}$$

$$d = 1-b_1b_2 < 0 \tag{1.5c}$$

are satisfied or not, five different scenarios of evolution, presented in figure 2, are possible. For brevity, a corresponding letter denotes that each of the inequalities (1.5) is satisfied, and an overbar means that the inequality is not satisfied. For example, $a\bar{b}c$ signifies that (1.5a) and (1.5c) are satisfied and (1.5b) is not satisfied. The regions where the C1–C3 states are stable are represented by heavy solid lines, and heavy dashes correspond to their instability region. The evolution with λ increasing and decreasing is shown by thin dashes with the arrows.

Based on this analysis we shall consider in §2 some particular models of a circular flow and shall determine what evolution scenarios of disturbances are possible in

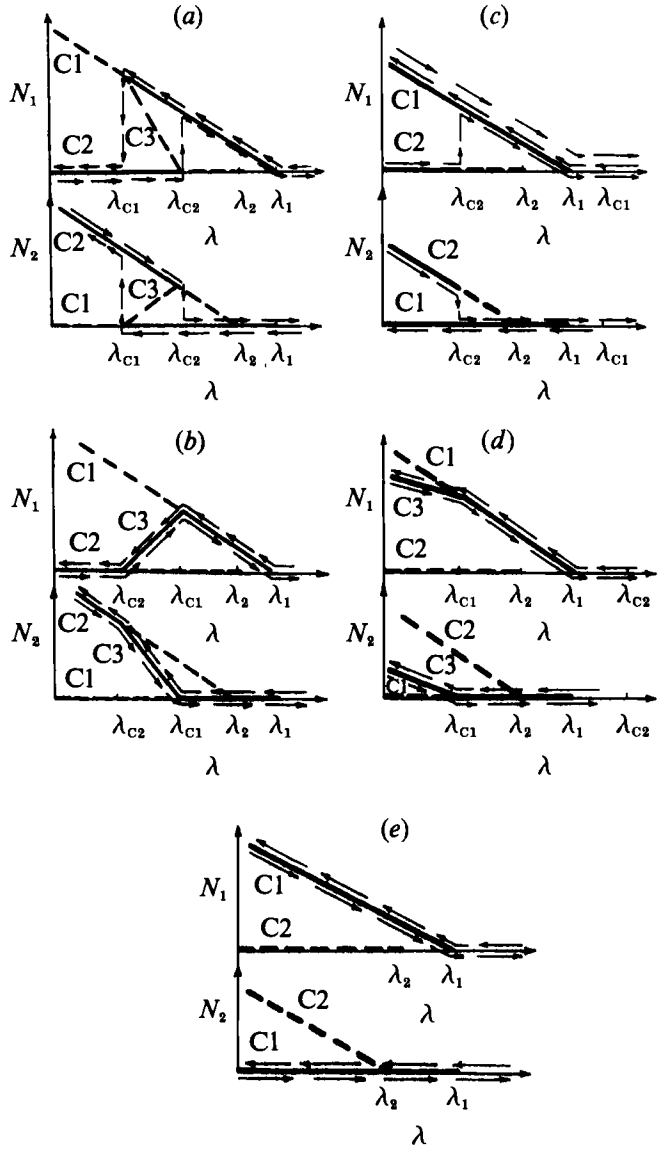

FIGURE 2. Possible variants of the evolution of the system (1.3).
(*a*) abc; (*b*) $ab\bar{c}$; (*c*) $\bar{a}bc$; (*d*) $ab\bar{b}\bar{c}$; (*e*) $\bar{a}\bar{b}c$ and $\bar{a}\bar{b}\bar{c}$.

terms of a weakly nonlinear two-modal model. Section 3 is devoted to a discussion of the results. Details of the derivation of the evolution equations are given in the Appendix.

2. Formulation of the problem; choice and calculation of the particular models

The diversity of the evolution scenarios admitted by equations (1.3) is commensurate with those observed experimentally, but the extent to which they are realized depends on the choice of the flow model. All scenarios in which mode 2 is excited in a direct cascade (with increasing supercriticality) require that the

inequality (1.5a) (see figure 2a,b,d) is satisfied; otherwise, only the excitation of fundamental mode 1 occurs in terms of (1.3).

For this reason, the simplest model of a plane shear layer, which is perhaps applicable if $L \ll R$ (R is the radius of the shear layer), is of no interest because (1.5a) is not satisfied in it. Indeed, in this case a disturbance with central wavenumber k is described by the nonlinear Schrödinger equation

$$\frac{\partial \psi}{\partial t} - a(\lambda_C - \lambda)\psi + \frac{a}{2}\frac{\partial^2 \lambda}{\partial k^2}\frac{\partial^2 \psi}{\partial x^2} + b|\psi|^2\psi = 0, \tag{2.1}$$

which, for the superposition of two modes $\psi = A_1 e^{iq_1 x} + A_2 e^{iq_2 x}$, is reduced to (1.2), (1.3). Since mode 1 is the first unstable one, or is close to it, it can be assumed that k corresponds to a maximum of $\lambda(k)$, and in this case the coefficients $b_1 = b_2 = 2$ and $a_1/a_2 = 1$ involved in (1.3) are such that only the $\bar{a}bc$ scenario (figure 2c) is realized, in which mode 2 can only be created artificially, outside the scope of the model (1.3).

Inequalities $\bar{a}bc$ in the model of a plane shear layer are satisfied definitely; therefore, the only way that mode 2 can be attained, hence enabling one to investigate the transition of one mode to another in terms of the approximation (1.3), is if the shear layer curvature is quite substantial, that is, the layer width L is of the order of its radius R: $D = L/R = O(1)$.

The flow will be described by two-dimensional incompressible hydrodynamics taking into account viscosity as well as Ekman friction. In polar coordinates r and ϕ we have

$$\frac{\partial}{\partial t}\nabla^2\tilde{\psi} + \{\nabla^2\tilde{\psi}, \tilde{\psi}\} + \tilde{\lambda}\nabla^2(\tilde{\psi} - \tilde{\psi}_{00}) = \nu\nabla^4(\tilde{\psi} - \tilde{\psi}_{00}). \tag{2.2}$$

Here $\tilde{\psi}$ is the stream function ($v_r = -r\,\partial\tilde{\psi}/\partial\phi$, $v_\phi = \partial\tilde{\psi}/\partial r$), $\tilde{\psi}_{00}$ is the stream function of an undisturbed flow, $\{a, b\} = [\nabla a, \nabla b]_z$, ν is the viscosity coefficient, and $\tilde{\lambda}$ is the coefficient of Ekman friction:

$$\tilde{\lambda} = \begin{cases} 8\nu/h^2 & \text{for flows under the lid,} \\ 2\nu/h^2 & \text{for flows without a lid,} \end{cases} \tag{2.3}$$

independently of the way, in which they are produced (it is anticipated that the thickness of the fluid layer h is much less than that of the Ekman layer h_E).

An undisturbed flow with a cylindrical layer of velocity shear lying at a distance R from the centre will be specified by the angular velocity profile

$$\Omega(r) = \tfrac{1}{2}(\Omega_1 + \Omega_2) - \tfrac{1}{2}(\Omega_1 - \Omega_2)\,u(r), \tag{2.4}$$

where $u(0) = -1$ and $u(\infty) = 1$, such that Ω_1 and Ω_2 are the respective angular velocities of the central part and the periphery. The calculations were carried out for the following u profiles: (a) $u = \tanh(y/D)$; (b) $u = 2/\pi \arctan(\pi y/2D)$; and ($c$) $u = (2/\pi)\arctan(p \sinh \pi y/2pD))$, where $y = \ln(r/R)$, and $D = L/R$ is the curvature parameter for the shear layer. When choosing the $u(y)$-profiles we took into consideration that (a) is actually a standard model of a shear layer, (b) differs from it by the slower (power-like) trend of u to ± 1 as $y \to \pm\infty$, which proves to be a factor; and finally, family (c) serves as a kind of a bridge between (a) and (b); also, if $p = 1$, profile (c) coincides with that calculated by Rabaud & Couder (1983) for their experiment.

The solution of (2.2) depends, apart from D, on a further parameter of the device, $\rho = Re_\lambda/Re$, where

$$Re = \frac{|\Omega_1 - \Omega_2|R^2 D}{\nu}, \quad Re_\lambda = \frac{|\Omega_1 - \Omega_2|}{2D\tilde{\lambda}} \tag{2.5}$$

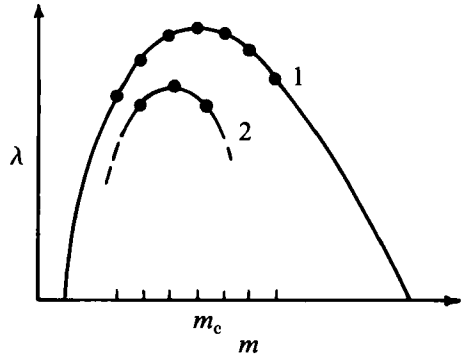

FIGURE 3. Neutral curve $\lambda = \lambda_m$ for a fixed D (schematically); curve 1, inviscid case; curve 2, viscous case.

are the 'viscous' and 'Ekman' Reynolds numbers. We shall use $\lambda = Re_\lambda^{-1}$ as the parameter that controls the disturbance evolution. In order to include flows produced both mechanically and by external forces, we investigate the solution of the complete equation (2.2) with $\rho = O(1)$ and of a shortened equation, with right-hand side set to zero (which corresponds to $\rho \to 0$), referring to these cases as viscous and inviscid respectively. The boundary conditions for $\psi = \tilde{\psi} - \tilde{\psi}_{00}$,

$$\psi = 0, \quad \partial\psi/\partial r = 0 \tag{2.6}$$

(the latter only in the viscous case), are imposed on the walls $r = r_1$ and $r = r_2$ ($r_1 < R < r_2$); the case $r_1 = 0$, $r_2 = \infty$ is also studied.

In terms of weakly nonlinear theory a solution of (2.2), (2.6) is sought in the form of an expansion in powers of the small parameter ϵ:

$$\psi = \epsilon\psi^{(1)} + \epsilon^2\psi^{(2)} + \epsilon^3\psi^{(3)} + \ldots, \tag{2.7}$$

with $\lambda - \lambda_l = \epsilon^2\lambda_l^{(1)}$ and $\lambda - \lambda_m = \epsilon^2\lambda_m^{(1)}$, where l and m are the azimuth mode numbers, whose interaction is examined. For a given D, the number of modes is limited by the condition $mD \lesssim 1$ such that $m_{\max} = O(D^{-1})$. Linear theory gives the stability boundary $\lambda = \lambda_n$, the growth rate $\gamma_n = a_n(\lambda_n - \lambda)$, the frequency

$$\omega(n) = \tfrac{1}{2}n(\Omega_1 + \Omega_2) - \alpha_n(\Omega_1 - \Omega_2) \tag{2.8}$$

and the eigenfunction g_n of each mode.

A typical plot of the n dependence of λ on m is presented in figure 3. A maximum value is reached when $m = m_C \sim \frac{1}{2}m_{\max}$. The value of α_m depends weakly on m (see tables 1–3 and figure 4*b*; cf. Rabaud & Couder 1983; Chomaz *et al.* 1988), and so the spectrum (2.3) seems to be non-decaying, i.e. there do not exist m, m_1, and m_2 such that the relationships

$$m = m_1 + m_2, \quad \omega(m) = \omega(m_1) + \omega(m_2)$$

are satisfied simultaneously. Therefore, the evolution equations contain a cubic (rather than quadratic) nonlinearity and, in the two-mode approach, have the form (cf. (1.2)):

$$\left.\begin{aligned} \frac{\mathrm{d}A_l}{\mathrm{d}t} &= a_l(\lambda_l - \lambda)A_l - \tilde{b}_{ll}|A_l|^2A_l - \tilde{b}_{lm}|A_m|^2A_l, \\ \frac{\mathrm{d}A_m}{\mathrm{d}t} &= a_m(\lambda_m - \lambda)A_m - \tilde{b}_{ml}|A_l|^2A_m - \tilde{b}_{mm}|A_m|^2A_m. \end{aligned}\right\} \tag{2.9}$$

(When comparing (2.9) with (1.2) and applying (1.5), it should be kept in mind that a mode with a larger value of λ_n corresponds to index 1.) The procedure for deriving (2.9) is a standard one; details are given in the Appendix.

In terms of weakly nonlinear theory one can only consider the interaction of a pair of modes for which $\lambda_l - \lambda_m = O(\epsilon^2)$. In the case of not too large m, this condition can be satisfied only with a suitable choice of D and only for the mode m_c and for those closest to it. Taking this into account, we take two neighbouring modes ($l = m+1$) as the pair l and m and for them find $D = D_m$ such that $\lambda_l = \lambda_m$; in this case $\lambda_m = \max_n(\lambda_n)$ automatically. Such a choice severely relates D to m: $D_m m = \text{const}$, so that a growth of m means a proportional decrease of the curvature parameter D. The necessary difference between λ_l and λ_m is attained by a small variation of D: positive ($\delta D = D - D_m > 0$) in the case $\lambda_l < \lambda_m$ and negative ($\delta D < 0$) if $\lambda_l > \lambda_m$. Taking δD into account (and, equivalently, taking into account the differences between λ, λ_l and λ_m) when calculating the coefficients a_i and $\tilde{b}_{ik}$ involved in (2.9), would be to exceed the accuracy. Results of the calculations are presented in tables 1–3 and in figures 4 and 5.

3. Results

3.1. *Inviscid flows* ($\rho \ll 1$; $r_1 = 0$, $r_2 = \infty$).

In the inviscid case, as is easy to see from (2.2), $\gamma_n = \lambda_n - \lambda$ such that all $a_n = 1$ and the inequalities (1.5*a*), (1.5*b*) are reduced to comparing $b_l = b_{lm}/b_{mm}$ and $b_m = b_{ml}/b_{ll}$ with unity ($b_{ik} = \mathrm{Re}\,(\tilde{b}_{ik})$). Table 1 gives the results for velocity profiles (*a*) $u = \tanh(y/D)$, (*b*) $u = 2/\pi \arctan(p \cdot \sinh \pi y/2\pi D)$, $p = 1$, and table 2 lists those for profiles. (*c*) $u = (2/\pi)\arctan(\pi y/2D)$, (*d*) $u = (2/\pi)\arctan(p \cdot \sinh \pi y/2pD)$, $p = 10$ which differ by a slower (power-like rather than exponential) trend of u to asymptotic values ± 1.† It is interesting to note that at the same m the shear layer in flows (*c*) and (*d*) has a larger width, and consequently, a larger curvature D. Figure 4 shows dispersion properties of flow model (*a*) for two values of D.

For each of flows (*a*)–(*d*), the inequalities

$$b_m < 1 < b_l \tag{3.1}$$

are satisfied (and for the first pair, $m = 2$, even $b_m \ll 1 \ll b_l$ are satisfied), which are equivalent to (1.5*a*), (1.5*b*) if a mode with a larger azimuthal number is taken as mode 1 (i.e. to make $m_c = l = m+1$, which requires $\delta D = D - D_m < 0$). This means that in each of these pairs, (2.9) admits transitions between the modes, and a direct cascade (transitions in the case of an increase in supercriticality) proceeds with decreasing m, and an inverse cascade is accompanied by an increase of m.

The inequality (1.5*c*) ceases to be satisfied only at the largest values of the curvature parameter D_m($m = 2$ in table 2). In this case both the direct and the inverse transitions proceed smoothly, through mixed state C3, with a gradual substitution of one mode by the other (figure 2*b*). In the other cases ($m = 2, 3$ in table 1 and $m = 3, 4$ in table 2), (1.5*c*) is satisfied, and the transition $m+1 \rightleftharpoons m$ proceeds abruptly and is, moreover, accompanied by hysteresis (figure 2*a*).

If, however, the mode m is taken as mode 1 ($m_c = m, \delta D > 0$), for the above first pairs we than have the scenario $\bar{a}\bar{b}c$ or $\bar{a}\bar{b}\bar{c}$ where the second mode is not excited at

† In flow (*d*), only the intermediate asymptotic representation ($1 < \pi y/2D < p$) has a power-like character.

	$u = \tanh(y/D)$				$u = (2/\pi)\arctan(p\sinh \pi y/2pD)$, $p = 1$			
m, l pairs	D_m λ_m	α_m α_l	b_m b_l	d	D_m λ_m	α_m α_l	b_m b_l	d
2, 3	0.2015	0.4732	0.339	−1.521	0.2086	0.4585	0.226	−0.953
	0.1607	0.4745	7.434		0.1571	0.4476	8.625	
3, 4	0.1350	0.4723	0.859	−2.960	0.1394	0.4560	0.762	−2.900
	0.1767	0.4725	4.611		0.1741	0.4487	5.117	
4, 5	0.1025	0.4717	1.162	−3.051	0.1057	0.4550	1.086	−3.085
	0.1822	0.4719	3.487		0.1800	0.4493	3.760	
5, 6	0.0828	0.4715	1.352	−3.007	0.0854	0.4543	1.300	−3.060
	0.1848	0.4716	2.963		0.1828	0.4498	3.130	
6, 7	0.0696	0.4714	1.479	−2.972				
	0.1862	0.4714	2.685					
10, 11	0.0427	0.4712	1.720	−2.951				
	0.1886	0.4712	2.298					
50, 51	0.0088	0.4711	1.952	−2.997	0.0091	0.4521	1.950	−3.00
	0.1896	0.4711	2.048		0.1879	0.4517	2.050	

TABLE 1. Results of calculations for inviscid flows for various values of m, l for two different velocity profiles.

	$u = (2/\pi)\arctan(\pi y/2D)$				$u = (2/\pi)\arctan(p\sinh \pi y/2pD)$, $p = 10$			
m, l pairs	D_m λ_m	α_m α_l	b_m b_l	d	D_m λ_m	α_m α_l	b_m b_l	d
2, 3	0.2730	0.3608	0.0473	0.501	0.2722	0.3619	0.0453	0.522
	0.1476	0.3339	10.56		0.1474	0.3348	10.57	
3, 4	0.1785	0.3584	0.616	−2.62	0.1778	0.3598	0.618	−2.63
	0.1683	0.3406	5.87		0.1682	0.3417	5.88	
4, 5	0.1342	0.3573	0.972	−3.09	0.1337	0.3587	0.971	−3.084
	0.1752	0.3438	4.21		0.1751	0.3449	4.21	
5, 6	0.1080	0.3565	1.20	−3.13	0.1076	0.3579	1.20	−3.13
	0.1784	0.3455	3.43		0.1783	0.3468	3.43	
6, 7	0.9095	0.3559	1.37	−3.10				
	0.1801	0.3467	3.00					
9, 10	0.0612	0.3548	1.63	−3.013				
	0.1823	0.3486	2.46					
50, 51	0.0114	0.3526	1.96	−2.997				
	0.1842	0.3514	2.04					

TABLE 2. As table 1 for two further velocity profiles.

all (figure 2*e*). Thus, whenever (2.9) admits transitions between the modes, they occur only in the region $m \leqslant m_C$, in total agreement with experiment.

At larger m the inequalities (3.1) are replaced by the inequalities

$$1 < b_m < 2 < b_{m+1}, \tag{3.2}$$

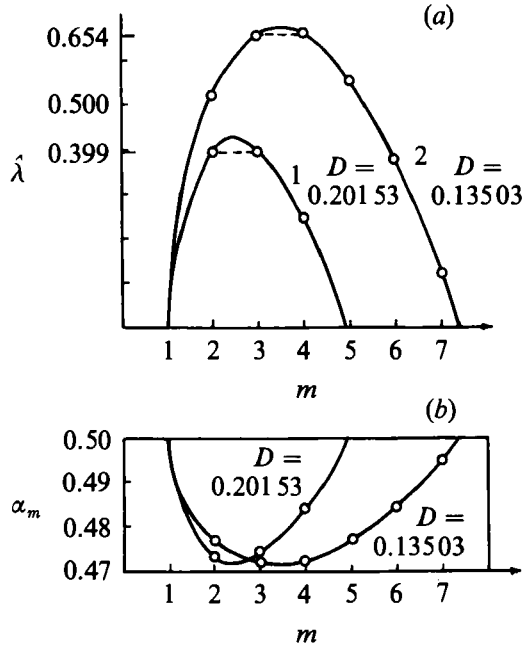

FIGURE 4. Dispersion properties of the flow model $u = \tanh(y/D)$ for two values of the parameter of curvature $D(\hat{\lambda} \equiv \lambda(2D)^{-1})$.

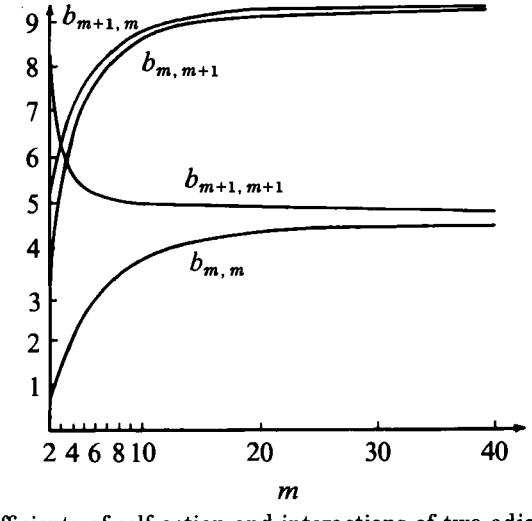

FIGURE 5. Coefficients of self-action and interactions of two adjacent modes for the model $u = \tanh(y/D)$.

which admit the only scenario $\bar{a}bc$ (figure 2*c*) as in the case of a plane shear layer. It is interesting to note that the transition b through 1 proceeds in different models with about the same D (though with different m), which, we believe, emphasizes the decisive influence of the shear-layer curvature upon the evolution scenarios of disturbances.

The dependence of the coefficients b_{ik} on m has a characteristic form and, for $u = \tanh(y/D)$, is plotted in figure 5, showing that when $D \to 0$ $(m \to \infty)$, $b_{ll} = b_{mm}$, $b_{lm} = b_{ml}$ and $b_{lm}/b_{mm} = b_1 = b_2 = 2$. In this limit the phase velocity of a disturb-

m, l pairs	D_m λ_m	α_m α_l	a_m a_l	b_m b_l	$\hat{b}_m$ $\hat{b}_l$	d
			$u = \tanh(y/D)$			
2, 3	0.1608	0.5483	1.262	1.069	1.218	−2.682
	0.1149	0.5616	1.438	3.443	3.022	
3, 4	0.1064	0.5538	1.283	1.376	1.497	−3.153
	0.1214	0.5614	1.395	3.018	2.775	
			$u = (2/\pi)\arctan(\pi y/2D)$			
2, 3	0.1665	0.4758	1.276	0.951	1.143	−2.468
	0.09654	0.4685	1.534	3.647	3.033	

TABLE 3. Results of calculations for viscous flows for two different velocity profiles; for $\hat{b}_m = a_l b_m / a_m$ and $\hat{b}_l = a_m b_l / a_l$, see (1.5*a*) and (1.5*b*).

ance $\omega(m)/m \to \frac{1}{2}(\Omega_1 + \Omega_2)$ and λ_m as a function of m looks like that shown in figure 3, and near the neutral curve maximum the approximation

$$\lambda = \lambda_m = \lambda_{\max} - \mu D^2 (m - m_C)^2$$

holds, where $\lambda_{\max} = 0.19$, $\mu = 3.1$, and $m_C = 0.45/D$. This agrees with the dependence of growth rate γ on wavenumber k obtained by Michalke (1964) for a plane layer, in view of the correspondence $\gamma \to \lambda_m$, $k \to mD$.

3.2. *Viscous flows* ($\rho = O(1)$)

The results of calculations for viscous flows without walls

$$(r_1 = 0,\ r_2 = \infty)\ u = \tanh(y/D) \quad \text{and} \quad u = (2/\pi)\arctan(\pi y/2D)$$

are presented in table 3. In the calculations we took $\rho = 0.5$. This corresponds to choosing $L = \frac{1}{2}h$ for a flow under the lid and to $L = h$ for a flow without a lid (see (2.3) and (2.5)). The first thing that attracts attention is the substantial difference of the dispersion properties from the inviscid flows properties: at the same m the value of D_m in a viscous flow is significantly smaller (see figure 3). As a consequence of this, in both models the inequality (1.5*a*) is not satisfied at any m, and the only possible scenario is $\bar{a}bc$ (figure 2*c*).

This conclusion is not altered if the sidewalls (r_1 and r_2 are finite) are taken into account. A calculation has shown that (1.5*a*), even for the first pair of modes ($m = 2$), can be satisfied only when they are very close to the shear layer ($|r_i - R|/R \lesssim 3D$) when the flow can no longer be considered two-dimensional.

3.3. *Discussion*

From the above analysis it is evident that the two-mode approach (1.3) is only suitable for describing transitions between modes with close stability thresholds ($\lambda_m - \lambda_l = O(\epsilon^2)$) in flows with sufficiently large curvature D of the shear layer for a sufficiently small supercriticality ($\lambda - \lambda_m = O(\epsilon^2)$). In this region of parameters the model is self-consistent because the admissible m is so small that even for modes neighbouring l and m we have $|\lambda_l - \lambda_m| \gg \epsilon^2$ (see figure 4*a*), and the behaviour it predicts (all transitions occur only when $m < m_C$ with hysteresis or through a mixed state) also roughly agrees with that observed experimentally. Unfortunately, however, the region itself is extremely narrow in the inviscid case and disappears

altogether in the viscous case (when $\rho = 0.5$). This may be why there are no experimental data pertaining to it directly (they are unknown to these authors, at least). It has been customary to investigate flows with $D < 0.1$ ($m = 5$–10 or more), for which the two-mode model gives only the scenario $\bar{a}bc$, allowing only for transitions with decreasing Re_λ which make m approach m_C ('lower' transitions, see figures 1 and 2*c*). The point here is that the two-mode model (1.3) is tenable only in the case of small supercriticality, i.e. in a narrow (in Re_λ) band near the neutral curve, and is unable to describe, at such small D values, the 'upper' transitions ($m \to m-1$ with increasing Re_λ) which proceed, as is evident from experiment, at large supercriticality ($Re^+_{\lambda m} - Re^-_{\lambda m} = O(Re_{\lambda m})$). For a correct description of the 'upper' transitions (direct cascade), it is necessary to include additional interactions, and experiment shows what they are. For example, Chomaz *et al.* (1988) found that in the case of even m the 'upper' transition is preceded by the excitation of a subharmonic ($\frac{1}{2}m$), and in the case of odd m it is preceded by the temporal mode.

The lower transitions are, we believe, quite well described in terms of weakly nonlinear theory, at least, at $|m - m_C|$ not too large.

We are grateful to Drs M. V. Nezlin and D. Yu. Manin for their stimulating interest in this work, and to the anonymous referees who pointed out the papers by Knobloch & Guckenheimer (1983) and Moroz & Holmes (1984). Thanks are also due to Mr V. G. Mikhalkovsky for his assistance in preparing the English version of the manuscript and for typing and retyping the text.

Appendix. The derivation of evolution equations (2.9)

If all variables are made dimensionless with the linear scale R and timescale $T = 2D/(\Omega_1 - \Omega_2)$, equation (2.2) for the flow (2.4) yields

$$\left(\frac{\partial}{\partial t} - \frac{u}{2}\frac{\partial}{\partial \phi} + \lambda\right)\tilde{\nabla}^2\psi + \tfrac{1}{2}(u'' + 2u')\frac{\partial \psi}{\partial \phi} + \{e^{-2y}\tilde{\nabla}^2\psi, \psi\} = \tilde{\nu}\tilde{\nabla}^2(e^{-2y}\tilde{\nabla}^2\psi) \qquad (A\,1)$$

where

$$\psi = (\tilde{\psi} - \tilde{\psi}_{00})\,TR^{-2}, \quad y = \ln\left(\frac{r}{R}\right), \quad \tilde{\nabla}^2 = \frac{\partial^2}{\partial y^2} + \frac{\partial^2}{\partial \phi^2},$$

$$\{a, b\} = \frac{\partial a}{\partial \phi}\frac{\partial b}{\partial y} - \frac{\partial a}{\partial y}\frac{\partial b}{\partial \phi}, \quad \tilde{\nu} = \rho\lambda D^2$$

and the prime denotes the derivative in y. Equation (A 1) in the inviscid ($\rho = \tilde{\nu} = 0$) and viscous ($\rho = 0.5$) cases was solved with the boundary conditions (2.6) on an unbounded ($-\infty < y < \infty$) interval and in the viscous case also on a bounded ($y_1 < y < y_2$) interval with the help of the expansion (2.7).

A. 1. *The linear approximation*: $O(\epsilon)$

Since we are concerned with the interaction of two (generally speaking) equivalent modes, then

$$\psi^{(1)} = A_l(\tau)\,g_l(y)\,e^{il\phi - i\omega(l)t} + A_m(\tau)\,g_m(y)\,e^{im\phi - i\omega(m)t} + \text{c.c.}; \quad \tau = \epsilon^2 t.$$

The function g_n satisfies, in the inviscid case, the second-order equation

$$\mathscr{L}^{(2)}_n g_n = \left(\frac{d^2}{dy^2} - \frac{u'' + 2u'}{u + 2\sigma_n/n} - n^2\right)g_n = 0, \qquad (A\,2)$$

and in the viscous case the fourth-order equation

$$\mathscr{L}_n^{(4)} g_n = \left\{\frac{\mathrm{d}^4}{\mathrm{d}y^4} - 4\frac{\mathrm{d}^3}{\mathrm{d}y^3} + \left[2(2-n^2) + \frac{\mathrm{i}n}{2\tilde{\nu}}\left(u + 2\frac{\sigma_n}{n}\right)\mathrm{e}^{2y}\right]\frac{\mathrm{d}^2}{\mathrm{d}y^2}\right.$$

$$\left. + 4n^2\frac{\mathrm{d}}{\mathrm{d}y} + n^2(n^2-4) - \frac{\mathrm{i}n}{2\tilde{\nu}}\left[u'' + 2u' + n^2\left(u + 2\frac{\sigma_n}{n}\right)\right]\mathrm{e}^{2y}\right\} g_n = 0, \quad \text{(A 3)}$$

where $\sigma_n = \omega_n + \mathrm{i}\lambda_n, \quad \omega_n = \omega(n) - n/2(\Omega_1 + \Omega_2), \quad n = l, m.$

At a given D each of (A 2) and (A 3) with corresponding boundary conditions is an eigenvalue problem whose solution determines ω_n and λ_n. Note that while in (A 2) these numbers are involved only as a common complex number σ_n, in (A 3) λ_n is also involved in $\tilde{\nu}$. The problem is solved for $n = m$ and $n = l = m+1$ to find $D = D_m$ such that $\lambda_l = \lambda_m$, and all subsequent calculations are performed with these D_m and λ_m. When calculating nonlinear terms, it is also convenient to use, along with g_n, the

$$P_n = \mathrm{e}^{-2y}\tilde{\nabla}^2 g_n \equiv \mathrm{e}^{-2y}\left(\frac{\mathrm{d}^2}{\mathrm{d}y^2} - n^2\right) g_n. \quad \text{(A 4)}$$

Also, since the operator $\mathscr{L}_n^{(4)}$ is not a self-conjugate one we shall need the eigenfunctions f_l and f_m of the problem conjugate to (A 3).

A. 2. *The quadratic approximation*: $O(\epsilon^2)$

The function of the second approximation

$$\psi^{(2)} = |A_l|^2 g_{0l} + |A_m|^2 g_{0m} + \{A_l^2 g_{2l}\,\mathrm{e}^{2\mathrm{i}l\phi - 2\mathrm{i}\omega(l)t} + A_m^2 g_{2m}\,\mathrm{e}^{2\mathrm{i}m\phi - 2\mathrm{i}\omega(m)t}$$
$$+ A_l A_m g_s\,\mathrm{e}^{\mathrm{i}(l+m)\phi - \mathrm{i}\omega(l)t - \mathrm{i}\omega(m)t} + A_l \bar{A}_m g_\delta\,\mathrm{e}^{\mathrm{i}(l-m)\phi - \mathrm{i}\omega(l)t + \mathrm{i}\omega(m)t} + \text{c.c.}\}$$

involves, along with the mean flow disturbance (through the zero harmonic), the second harmonics of each of the modes, and the sum (g_s) and difference (g_δ) harmonics (the bar denotes complex conjugation).

All harmonics, except the zero harmonic, are calculated in the same fashion. The equation

$$\mathscr{L}_n^{(2)} g_n = R_n/(\sigma_n + \tfrac{1}{2}nu)$$

is solved in the inviscid case, or

$$\mathscr{L}_n^{(4)} g_n = \mathrm{i}R_n\,\mathrm{e}^{2y}/\tilde{\nu}$$

in the viscous case, where

$$n = 2m,\ 2l; \quad s = l+m; \quad \delta = l-m;$$

$$\sigma_{2m} = 2\omega_m + \mathrm{i}\lambda, \quad \sigma_{2l} = 2\omega_l + \mathrm{i}\lambda, \quad \sigma_s = \omega_l + \omega_m + \mathrm{i}\lambda, \quad \sigma_\delta = \omega_l - \omega_m + \mathrm{i}\lambda,$$

$$R_{2m} = m(P_m g_m' - P_m' g_m); \quad R_{2l} = l(P_l g_l' - P_l' g_l);$$

$$R_s = l(P_l g_m' - P_m' g_l) + m(P_m g_l' - P_l' g_m);$$

$$R_\delta = l(P_e \bar{g}_m' - \bar{P}_m' g_l) - m(\bar{P}_m g_l' - P_l' \bar{g}_m).$$

Zeroth harmonics in the inviscid case are obtained immediately in explicit form:

$$g_{0n}' = -\frac{\mathrm{i}n}{\lambda}(P_n \bar{g}_n - \bar{P}_n g_n), \quad n = l, m,$$

and in the viscous case as the solution of the equation

$$\mathscr{L}_0^{(4)} g_{0n} = \frac{in}{\tilde{\nu}} e^{2y} \frac{d}{dy}(P_n \bar{g}_n - \bar{P}_n g_n), \quad n = l, m,$$

with the conditions $g_{0n} = 0$ and $g'_{0n} = 0$ on the boundaries. For subsequent calculations, we shall need, as well as g_i, also P_i specified by (A 4).

A. 3. *The cubic approximation*: $O(\epsilon^3)$

In this order we are interested only in corrections to the lth and mth harmonics caused by the non-stationarity, the difference between λ, λ_l, and λ_m, and by the nonlinearity

$$\psi^{(3)} = \psi_l^{(3)} + \psi_m^{(3)}.$$

In the inviscid case

$$\mathscr{L}_l^{(2)} \psi_l^{(3)} = -\frac{i}{\sigma_l + \frac{1}{2} l u} \left\{ \left(\frac{\partial A_l}{\partial \tau} + \lambda_l^{(1)} A_l \right) P_l e^{2y} + |A_l|^2 A_l R_{ll} + |A_m|^2 A_l R_{lm} \right\}$$

and in the viscous case

$$\mathscr{L}_l^{(4)} \psi_l^{(3)} = \frac{e^{2y}}{\tilde{\nu}} \left\{ \left(\frac{\partial A_l}{\partial \tau} + \lambda_l^{(1)} A_l \right) P_l e^{2y} - \rho D^2 \lambda_l^{(1)} A_l \left(\frac{d^2}{dy^2} - l^2 \right) P_l + |A_l|^2 A_l R_{ll} + |A_m|^2 A_l R_{lm} \right\},$$

and similarly for the mth mode; we shall not give the explicit expressions for R_{ik} here because they are too unwieldy. By multiplying each of the equations obtained by the eigenfunction of the corresponding conjugate problem and integrating, we obtain the evolution equation (2.9).

REFERENCES

Chomaz, J. M., Rabaud, M., Basdevant, C. & Couder, Y. 1988 Experimental and numerical investigation of a forced circular shear layer. *J. Fluid Mech.* **187**, 115–140.

Dolzhanskiĭ, F. V., Krymov, V. A. & Manin, D. Yu. 1990 Stability and vortex structures in quasi two-dimensional shear flows. *Usp. Fiz. Nauk* **160** (7), 1–47 (in Russian).

Dovzhenko, V. A. & Krymov, V. A. 1987 An experimental study of the stability of zonal shear flows in circular geometry. *Izv. Akad. Nauk SSSR. Fiz. Atmos. i Okeana* **23** (1), 14–20 (in Russian).

Drazin, P. G. 1972 Nonlinear baroclinic instability of a continuous zonal flow of viscous fluid. *J. Fluid Mech.* **55**, 577–587.

Knobloch, E. & Guckenheimer, J. 1983 Convective transitions induced by a varying aspect ratio. *Phys. Rev.* A **27**, 408–417.

Krymov, V. A. 1988 Experimental investigation of supercritical vortical regimes in axisymmetric shear flow. *Izv. Akad. Nauk SSSR. Fiz. Atmos. i Okeana.* **24** (5), 475–482 (in Russian).

Lotka, A. J. 1925 *Elements of Physical Biology.* Baltimore: Williams & Wilkins.

Michalke, A. 1964 On the inviscid instability of the hyperbolic-tangent profile. *J. Fluid Mech.* **19**, 543–556.

Moroz, I. M. & Holmes, P. 1984 Double Hopf bifurcation and quasi-periodic flow in a model of baroclinic instability. *J. Atmos. Sci.* **41**, 3147–3160.

Nezlin, M. V., Rylov, A. Yu., Trubnikov, A. S. & Khutortskii, A. V. 1990 Cyclonic–anticyclonic asymmetry and a new soliton concept for Rossby vortices in the laboratory, oceans and the atmospheres of giant plants. *Geophys. Astrophys. Fluid Dyn.* **52**, 211–247.

Nezlin, M. V. & Snezhkin, E. N. 1990 *Rossby Vortices and Spiral Structures.* Moscow: Nauka, (in Russian).

NIINO, H. & MISAWA, N. 1984 An experimental and theoretical study of barotropic instability. *J. Atmos. Sci.*, **41**, 1992–2011.

PEDLOSKY, J. 1979 *Geophysical Fluid Dynamics.* Springer.

RABAUD, M. & COUDER, Y. 1983 A shear flow instability in circular geometry. *J. Fluid Mech.* **136**, 291–319.

SEGEL, L. A. & STUART, J. T. 1962 On the question of the preferred mode in cellular thermal convection. *J. Fluid Mech.* **13**, 289–306.

VOLTERRA, V. 1931 *Lecons sur la Theorie Mathematique de la Lutte pour la Vie.* Gauthier-Villars.